Figure 1. Representation of the emulators for pairs of parameters with other parameters fixed at their nominal values. Results are under the weakly nonlinear sliding law. Emulators (**a**) at 2100 in RCP 2.6 for the pair $(F_{\mathrm{calv}}, E_{\mathrm{shelf}})$, (**b**) at 2300 in RCP 8.5 for the pair $(F_{\mathrm{melt}}, E_{\mathrm{shelf}})$, (**c**) at 2300 in RCP 2.6 for the pair $(F_{\mathrm{calv}}, F_{\mathrm{melt}})$ and (**d**) at 3000 in RCP 2.6 for the pair $(F_{\mathrm{melt}}, E_{\mathrm{shelf}})$.
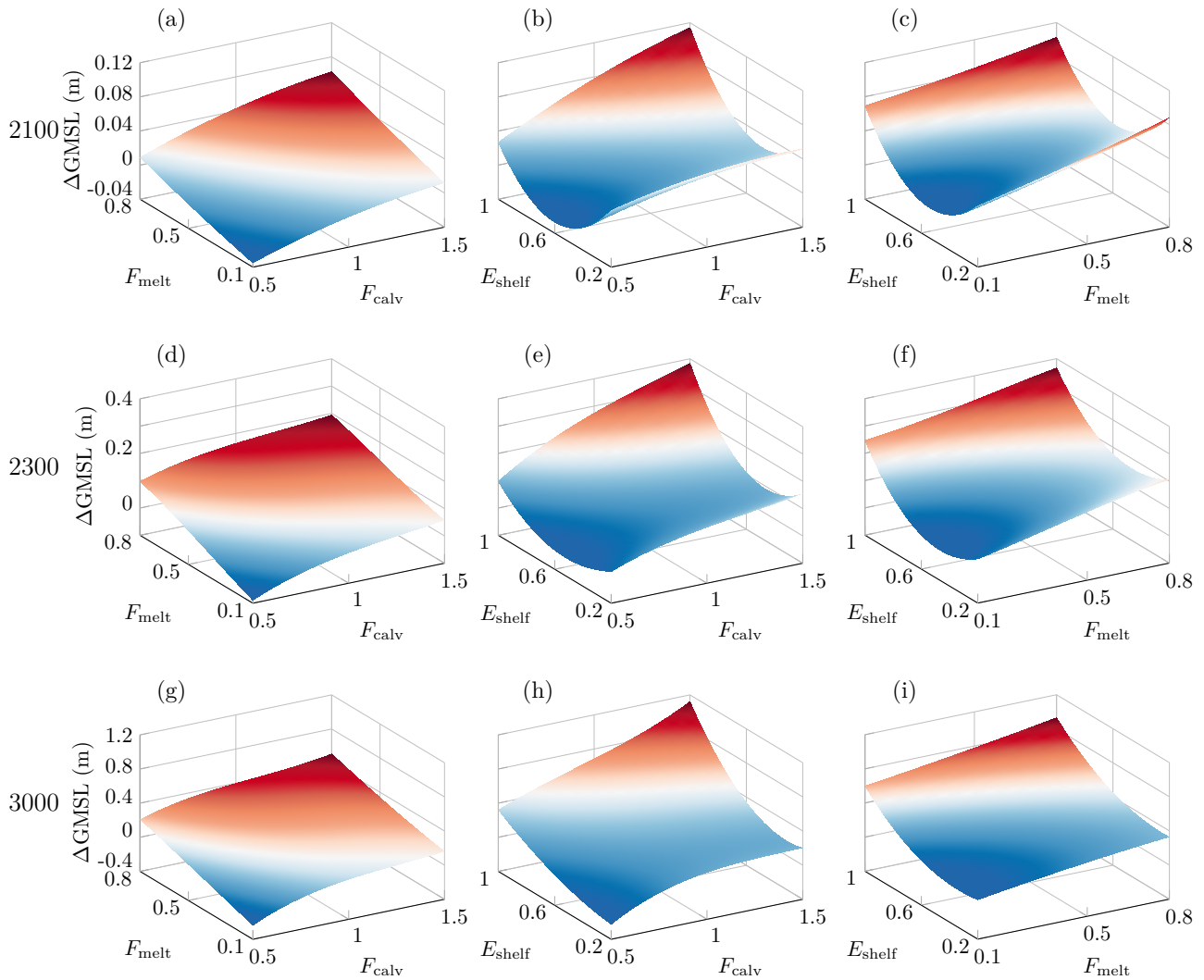
Figure 2. Representation of the emulators for pair of parameters with other parameters fixed at their nominal values. Results are for the RCP 2.6 scenario under the weakly nonlinear sliding law. Emulators at 2100 (**a**,**b**,**c**), emulators at 2300 (**d**,**e**,**f**) and emulators at 3000 (**f**,**g**,**i**).
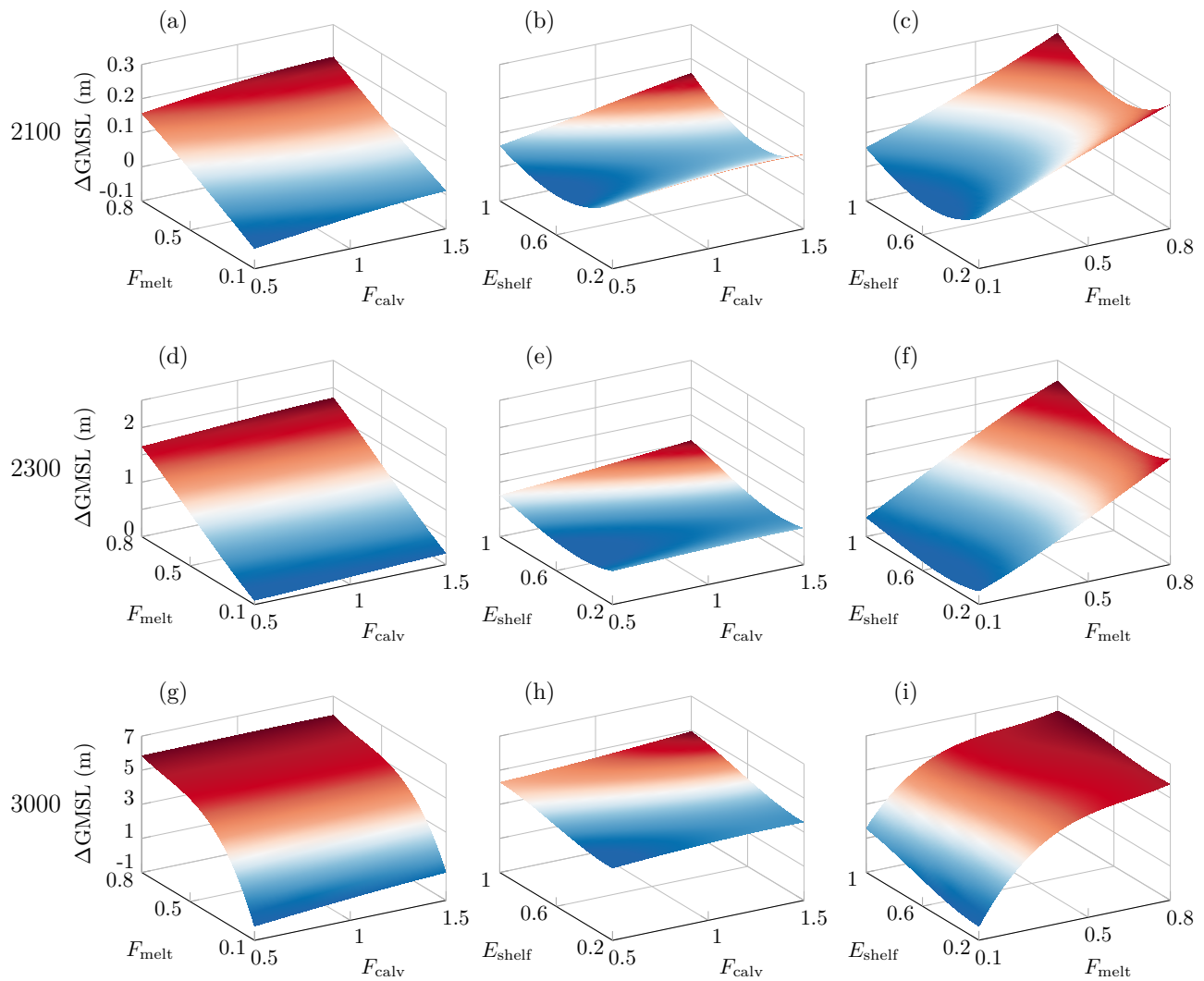
Figure 3. Representation of the emulators for pair of parameters with other parameters fixed at their nominal values. Results are for the RCP 8.5 scenario under the weakly nonlinear sliding law. Emulators at 2100 (**a**,**b**,**c**), emulators at 2300 (**d**,**e**,**f**) and emulators at 3000 (**f**,**g**,**i**).
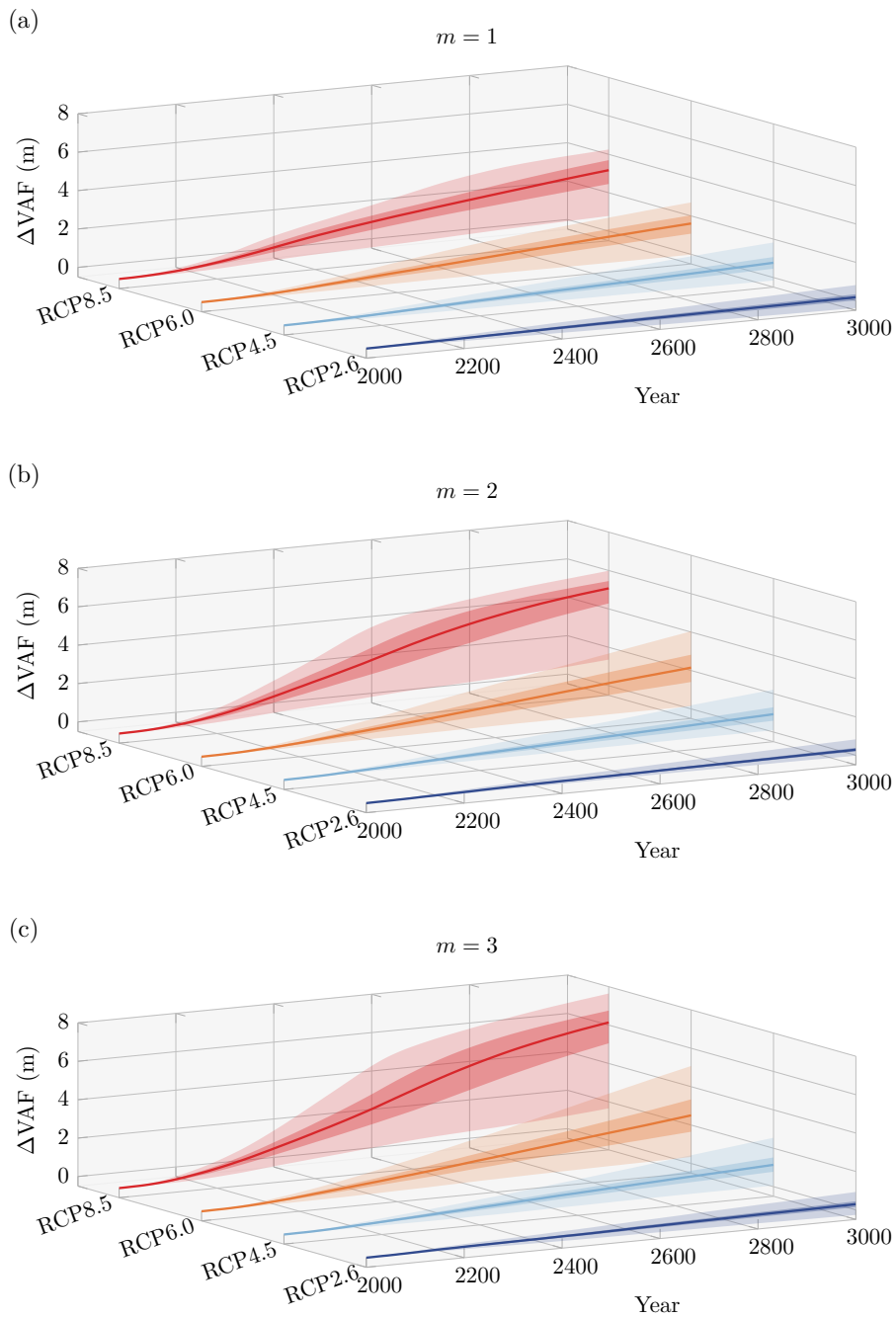
Figure 4. Antarctic ice-sheet contribution to global mean sea level relative to 2000. (**a**) Viscous sliding law, (**b**) weakly nonlinear sliding law and (**c**) strongly nonlinear sliding law. Solid lines are the median projections, the darker and lighter shaded areas are respectively the medium and very high probability intervals (33–66 % quantiles and 5-95 % quantiles) that represent the parametric uncertainty in the model.
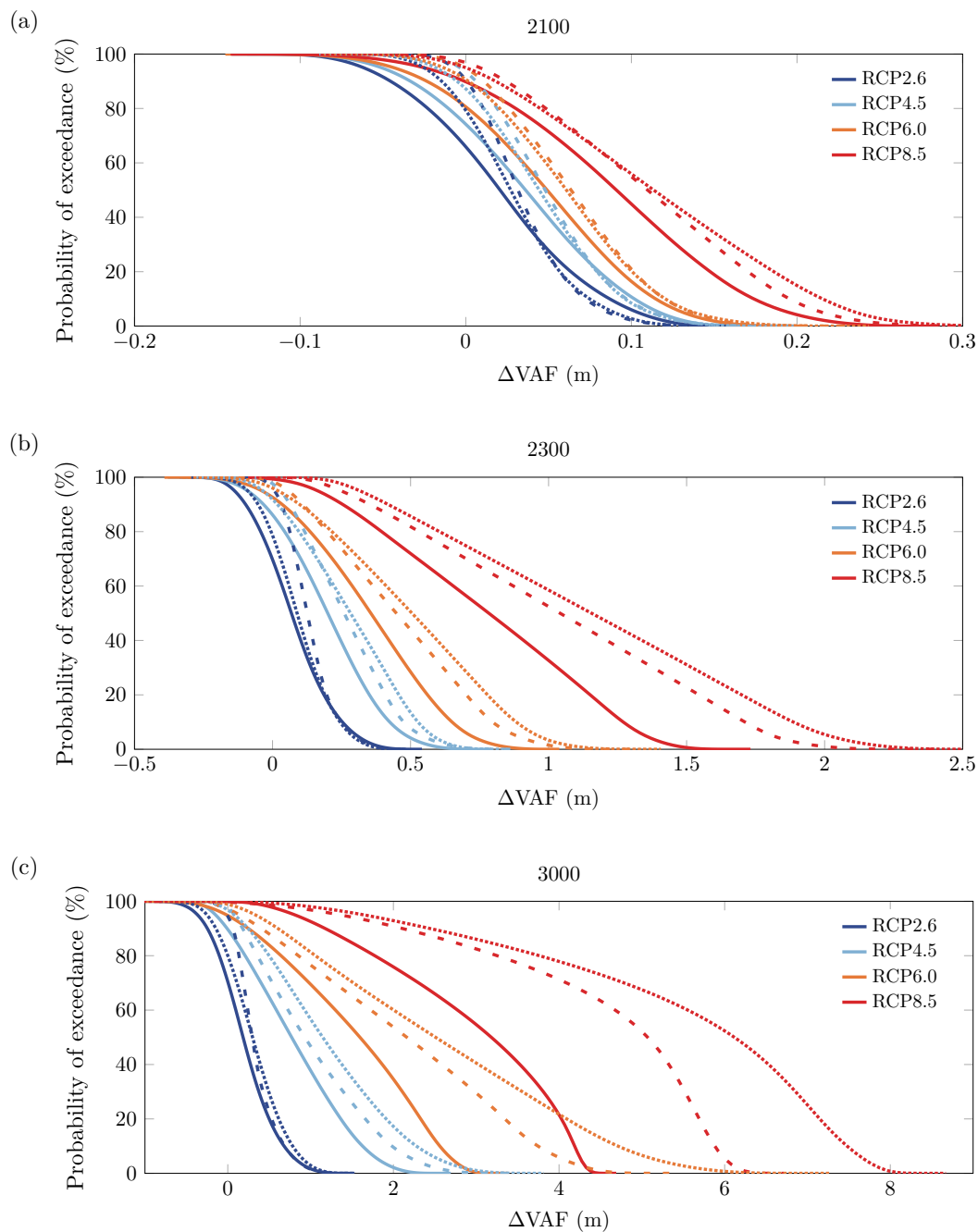
Figure 5. Probability of exceeding threshold values for sea-level rise evaluated as the complementary cumulative distribution functions of the probability density functions for sea-level rise projections. Probability of exceedance at 2100, (**b**) at 2300 and (**c**) at 3000. Solid lines are projections under the viscous sliding law, dashed lines are projections under the weakly nonlinear sliding law and dotted lines are projections under the strongly nonlinear sliding law.

	2100	2300	3000
RCP2.6	(a)	(b)	(c)
RCP4.5	(d)	(e)	(f)
RCP6.0	(g)	(h)	(i)
RCP8.5	(j)	(k)	(l)

Probability to remain grounded

100%   ⩾95%   ⩾66%   ⩾50%   ⩾33%   ⩾5%   ⩾0%
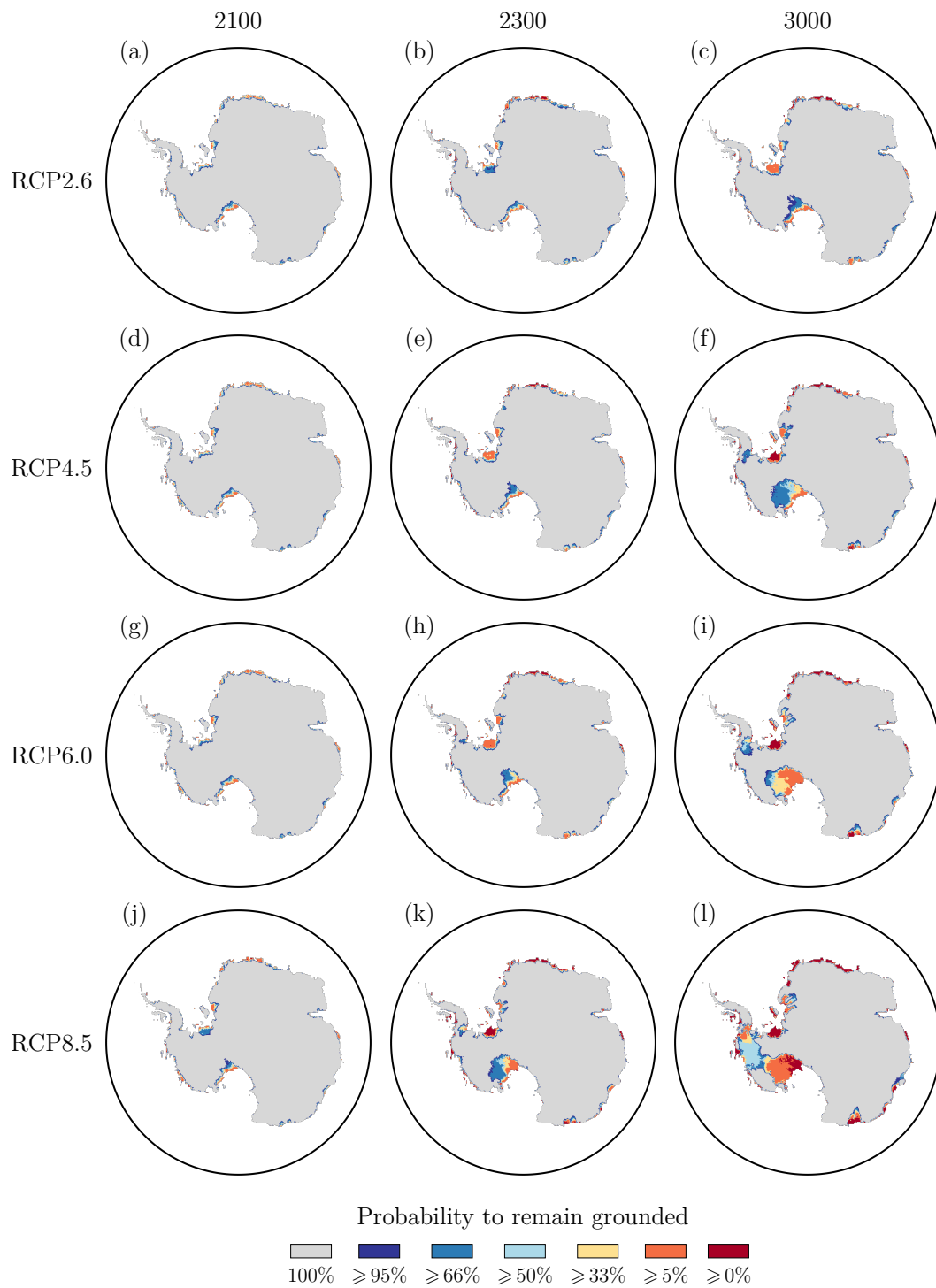
Figure 6. Confidence regions for grounded ice in all RCP scenarios under the viscous sliding law. Confidence regions are shown at 2100 (**a**, **d**, **g**, **j**), 2300 (**b**, **e**, **h**, **k**) and 3000 (**c**, **f**, **i**, **l**).
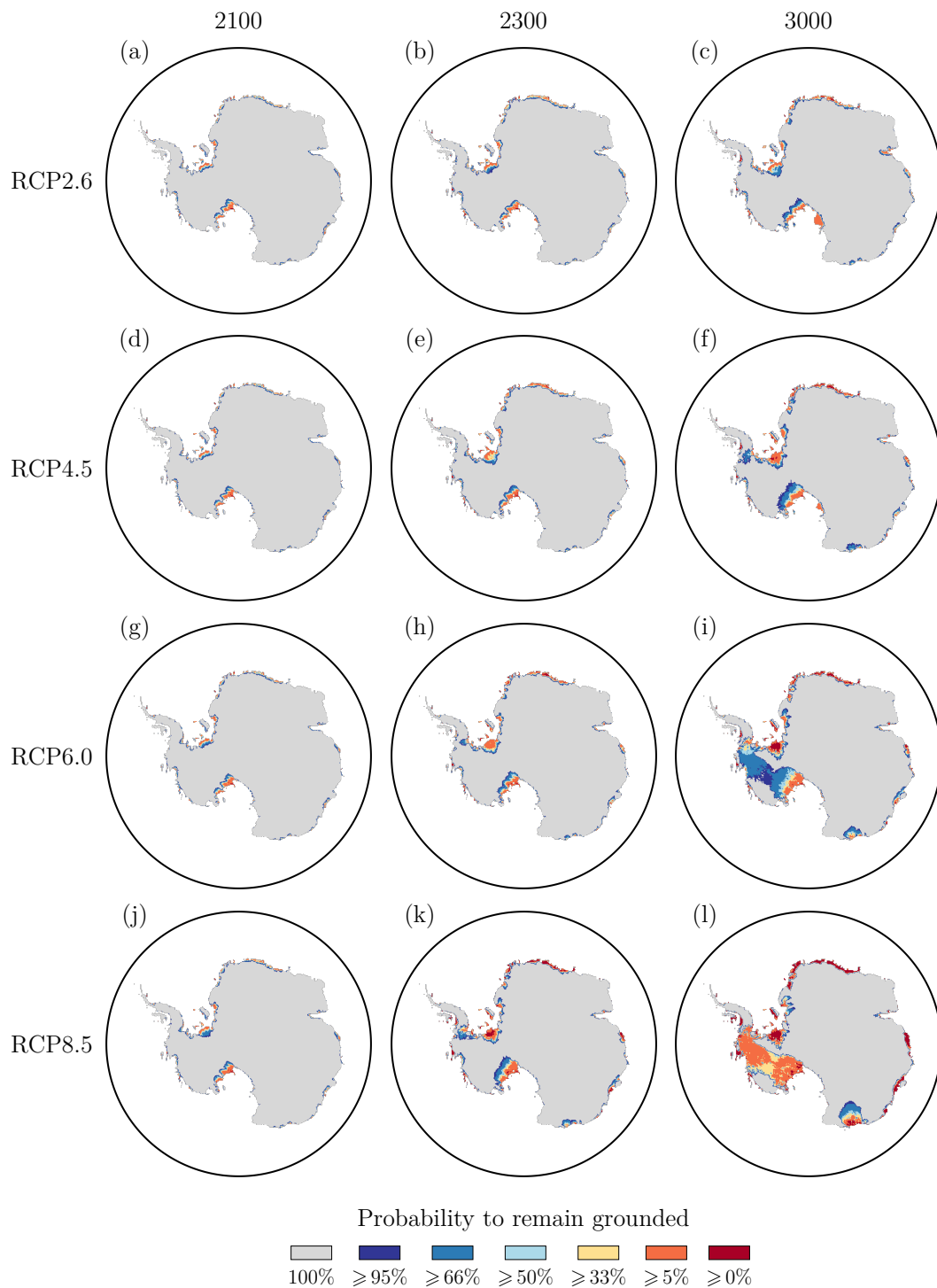
Figure 7. Confidence regions for grounded ice in all RCP scenarios under the strongly nonlinear sliding law. Confidences region are shown at 2100 (**a**, **d**, **g**, **j**), 2300 (**b**, **e**, **h**, **k**) and 3000 (**c**, **f**, **i**, **l**).
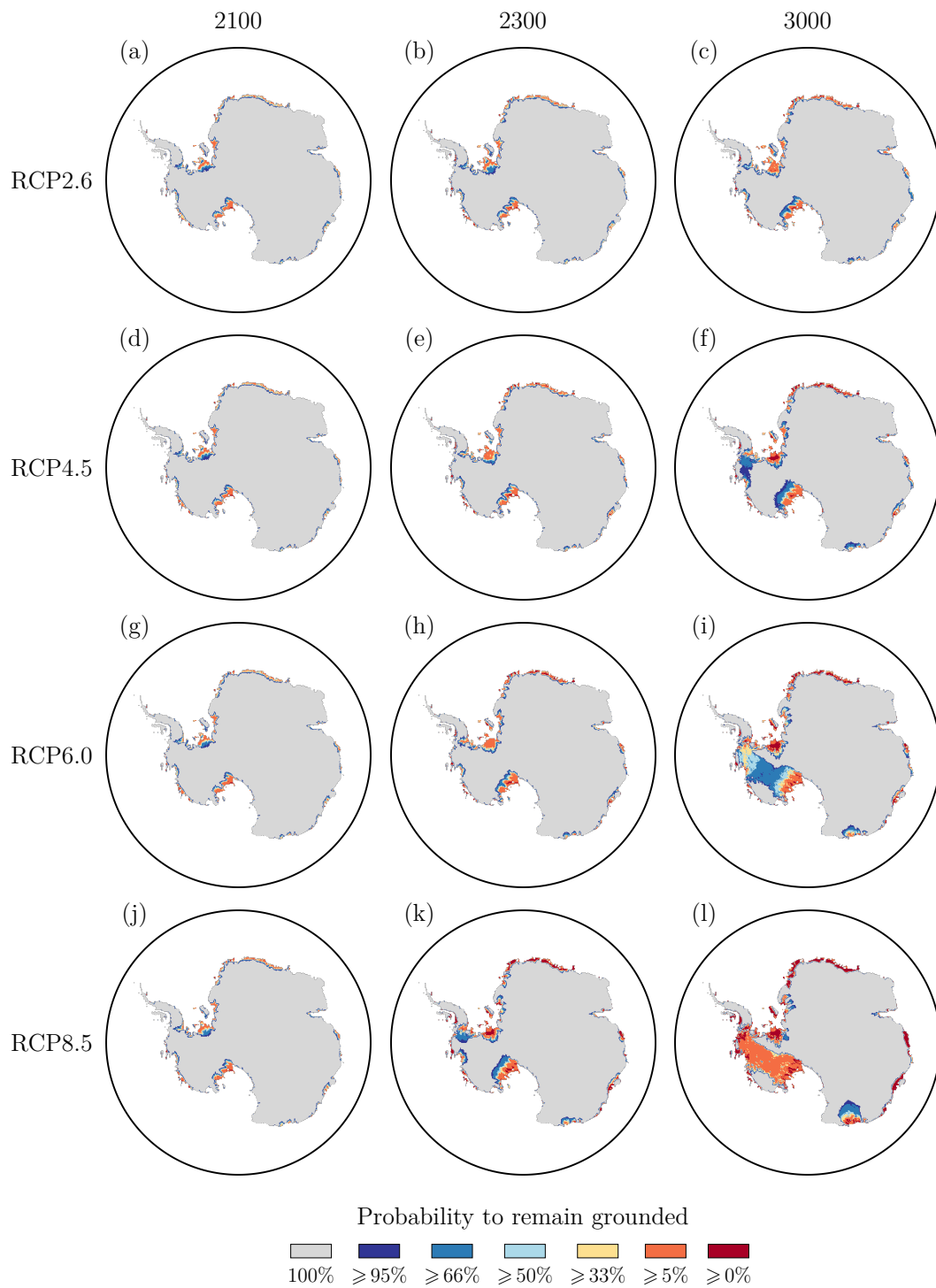
Figure 8. Confidence regions for grounded ice in all RCP scenarios under sliding law with exponent $m = 5$. Confidences region are shown at 2100 (**a**, **d**, **g**, **j**), 2300 (**b**, **e**, **h**, **k**) and 3000 (**c**, **f**, **i**, **l**).
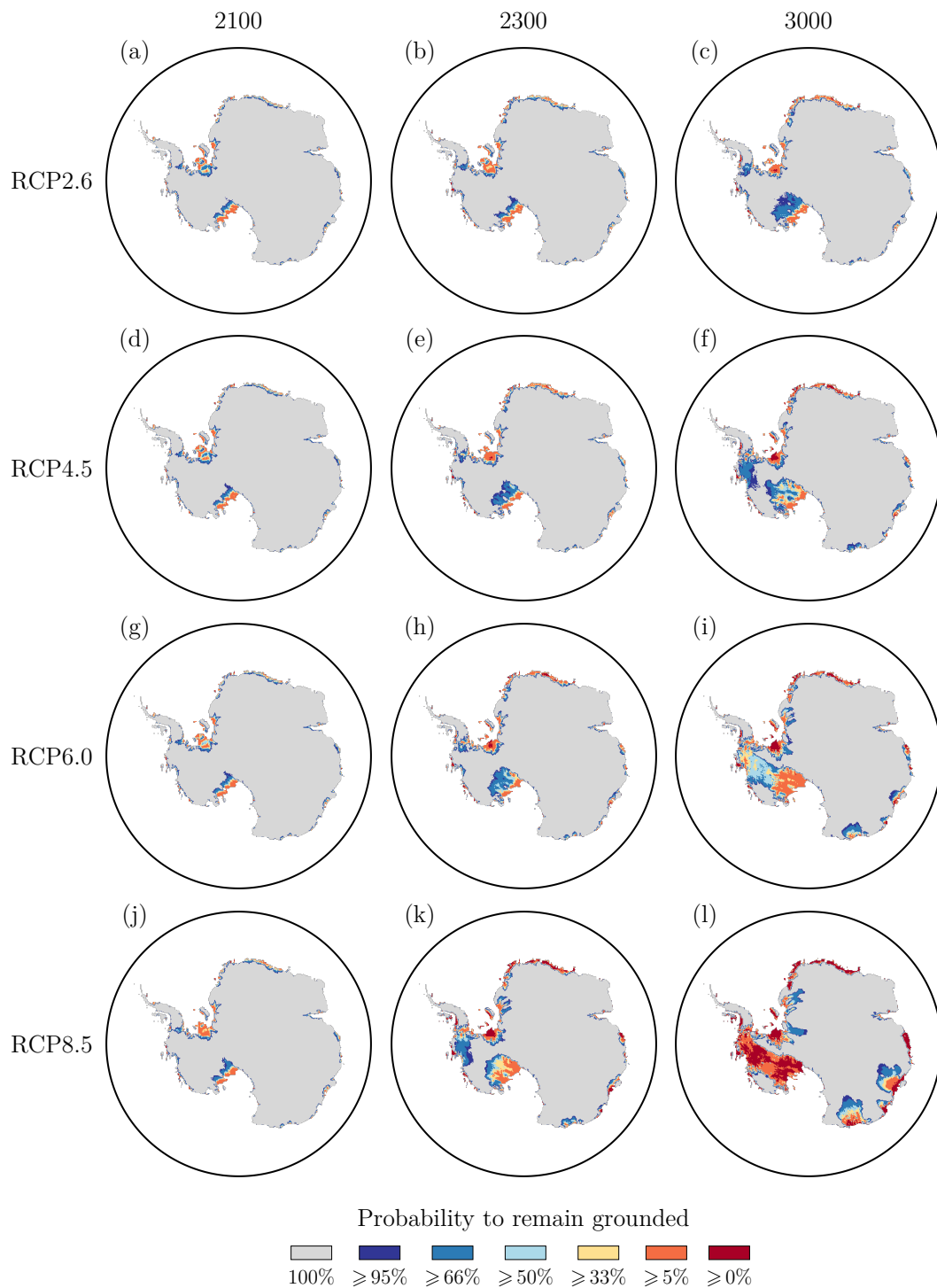
Figure 9. Confidence regions for grounded ice in all RCP scenarios under the weakly nonlinear sliding law and TGL parameterisation. Confidence regions are shown at 2100 (**a**, **d**, **g**, **j**), 2300 (**b**, **e**, **h**, **k**) and 3000 (**c**, **f**, **i**, **l**).